




Revolutionizing Sports Training with Collaborative CAD Multimedia Technology Demonstrations

Chungen Zhang^{1*} 

¹JiangXi University of Engineering, Xinyu, Jiangxi, 338000, China

Corresponding Author: Chungen Zhang, zhangcgjx00@163.com

Abstract. To improve the demonstration effect of sports training, it studies the demonstration method of sports training combined with multimedia technology. It proposes a new method of point cloud segmentation based on the principal component feature ball. According to the process of local feature analysis of point clouds, this paper first divides point clouds into surface objects, linear points, and circular points. Through the normal clustering and location segmentation of surface objects, this paper proposes a new method of point cloud fragment fusion, which achieves the segmentation of the entire scene by merging non-ground fragments to complete non-ground object segmentation. Finally, this paper verifies that the sports training demonstration method based on multimedia is very effective through multiple groups of sports training simulations.

Keywords: multimedia technology; sports; training; demonstration method; Collaborative CAD

DOI: <https://doi.org/10.14733/cadaps.2025.S5.59-74>

1 INTRODUCTION

In the construction of modern information technology software and hardware, it is necessary to focus on cultivating teachers' quality education on modern information technology so that more teachers can learn to apply modern information technology. Moreover, educational institutions should appropriately provide education funds to teachers. If conditions permit, a training base can be established. Through formal training and guidance, teachers and trainers can fundamentally recognize the importance of modern information technology in teaching and training and gradually become proficient in operating procedures and means of use through practice. In the process of competition, we must learn to understand and tolerate each other, jointly promote the progress of modern information technology, and make teachers and trainers play a calling role for modern information technology in training [1].

Training adaptation is the biological basis for the continuous improvement of human function: the continuous improvement of human function is one of the important tasks of sports training, and

the continuous improvement of human function depends on the process of training adaptation. The training adaptation of the body to muscle activities is manifested in the minimum energy consumption and the minimum damage to the internal environment, as well as maintaining a good balance of muscle energy and material to ensure the completion of training tasks [2]. That is to say, the work that needed great effort before can be completed now only needs small efforts. At this time, the body can bear more exercise load and show better body capacity. Training adaptation is the biological basis for developing a competitive state: the formation of a sports competitive state is the result of a highly developed training adaptation process. The formation of a competitive state requires athletes to achieve a relatively perfect degree of training adaptation in the form, function, quality, technology, tactics and psychological state of each organ system and combine them harmoniously into a whole [3]. The temporary disappearance of the competitive state is the result of the anti-adaptive decline of training. This kind of anti-adaptive decline enables athletes to recover their bodies, develop new training adaptations further, reform the competitive state at a higher level, and achieve better sports results. Training adaptation is the biological basis of sports training theory; sports training theory is the summary and generalization of sports practical experience. It is based on the objective laws of sports training and plays a guiding role in sports training practice. Only on the basis of training adaptation and other objective laws of sports training can sports training theory be tested by sports training practice, form a scientific theoretical system, and guide sports training to develop in the right direction [4].

Adaptation refers to the permanent changes in human function and shape under the influence of long-term changes in the environment. When the external environment changes, the relative balance of the internal environment is destroyed, and various functions in the body have to be readjusted to maintain the relative balance of the internal environment, which is the adaptation process. In sports training, the method of imposing sports load is mainly used to intentionally break the relative balance of the internal environment of the machine so that it can be transformed to a higher functional level so that the relative balance can be regained at the level appropriate to the imposed sports load [5]. This process of constantly balancing the organism generated by sports training with the external environment of the load is called training adaptation. The essence of training adaptation can be said to be that, on the one hand, it can improve or reduce the sensing threshold of the nervous system and other tissues and organs to stimuli. On the other hand, it also enhances the compensatory function of the body. The adjustment of the training adaptation process is mainly carried out through the neurohumoral pathway. Through the improvement of the function of this pathway, the body will have the above adaptive changes [6]. The universality of training adaptation refers to the phenomenon that the body can adapt to training in terms of shape, function, sports quality, techniques and tactics, and psychological process. The particularity of training adaptation refers to the different nature of exercise load, which can cause special adaptation changes. It is commonly understood that what you practice is what you grow [7]. The different times of training adaptation refer to the adaptive change of the body due to sports training requiring a certain time, and the time of the occurrence of various aspects of the training adaptation phenomenon of the body is also different. The functional adaptive change often precedes the structural adaptive change. The continuity of training adaptation means that the emergence and development of the body training adaptation is a continuous process. Because the training adaptation of the body in various competitive abilities has the characteristics of different times, it leads to the formation of the body's overall adaptation in the way of gradual accumulation [8]. Literature [9] believes that "the body adaptation caused by the stimulation of training load to the body is not permanent. When the training stops, the body lacks the necessary stimulus conditions, which leads to the regression and loss of training adaptation". "The adaptation of the neuromuscular system to sports is a very important part of training adaptation. The nervous system is the control system, and the muscle is the effect system. Both of them cooperated reasonably to complete the technical action. The adaptation of the neuromuscular system to sports training has a wide range of

manifestations". "The spiritual adaptation is not easy to fade". Literature [10] believes that sports training has a specialized effect. Each kind of sports exercise determines different levels of activity in different organs, different types of muscles and different sports units. Different training characteristics determine different metabolic pathways required to complete different functional tasks in various active cells, as well as metabolic control systems and body function regulation systems at various levels. Therefore, different types and characteristics of systematic exercise will leave different adaptive characteristics in different tissues and organs. Literature [11] mentions that sports training is a science, and its scientific nature lies in the fact that training arrangements must be highly consistent with the changing laws of human physiological functions. Sports training is also an art. Its artistry lies in the reasonable arrangement of various elements of sports training (load intensity, duration, amount of exercise, recovery method, etc.) so that the body can produce the best response and adaptation, that is, to produce the maximum effect of sports training. According to the literature [12], the physiological essence of exercise training is: 1. The essence of exercise load, stimulus-response, and the essence of exercise load is also an external stimulus and a very strong stimulus, which will lead to very severe responsive changes in the body. 2. The influence of sports training: the destruction and reconstruction of structure and function. 3. Improvement of sports ability: long-term stimulation adaptation. In essence, the long-term sports training process is a repeated stimulation reaction adaptation process, which is a cycle process of continuous destruction and reconstruction of body structure and function. Through this cycle, sports ability and performance are constantly enhanced.

The formation of motor skills is related to learning and memory. As input information, training load stimulation acts on neurons through afferent nerves, changes in membrane potential, release of neurotransmitters, and modification of synapses. Neurons interact with each other to form short-term memory and long-term memory. This learning process is self-organized. The learning of motor skills, first of all, forms the plastic changes of synaptic efficacy corresponding to the spatiotemporal order of actions through the transmission of neural information [13]. On this basis, the plasticity of the synaptic effect can be changed by intensive training. Once the synaptic morphology changes, the learned behavior is not easy to fade or forget. If you haven't swum for many years after learning to swim, you will never forget it. Habitual behavior is difficult to change; A mistake that seems to have been corrected sometimes occurs spontaneously, and so on. Therefore, for a new skill, in order to achieve a certain amount of intensive training, we should not simply stop or just be satisfied with learning it. At the same time, we should ensure that the right motor skills are acquired to strengthen, thereby inducing the plasticity or morphological changes of the synaptic efficacy of the corresponding motor skills [14]. Studies have shown that to establish and consolidate synapses, there must be neural activity. Inactive or less active synapses will be eliminated, and neurons that fail to establish synaptic connections will die. This, in a sense, explains why complex sports skills should be trained and cultivated from an early age. From the perspective of intellectual development, there is a critical period for the development of many abilities. In addition to the mature factors, the degradation of synapses and the death of neurons that have not been trained to establish neural connections may be important reasons [15]

This paper combines multimedia technology to study the demonstration method of sports training to improve the effect of sports training.

2 FEATURE RECOGNITION FOR SPORTS TRAINING PRESENTATIONS

2.1 Driver Layer

The point cloud data collection process communicates with the 3D laser scanning rangefinder in real-time and is responsible for the collection of 3D point cloud data. There are two asynchronously running threads in this process: the point cloud data collection thread and the data writing thread.

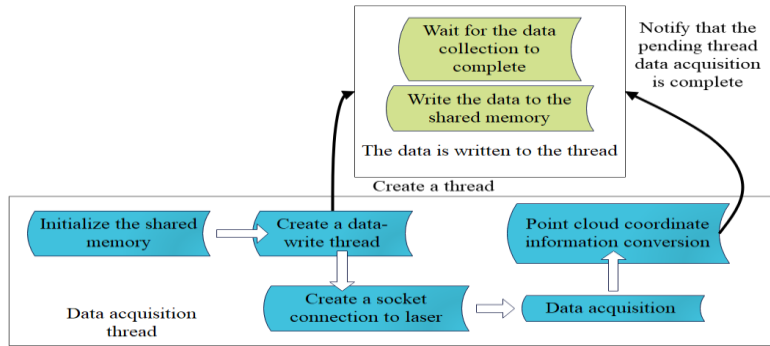


Figure 1: Flowchart of the point cloud collection process.

The Velodyne VLP-16 3D laser rangefinder is a 16-line laser, and the 16-line laser beam is distributed in the vertical direction. When the 3D laser rangefinder collects the point cloud, the 3D information of 16 points can be obtained in space by each step of rotation. The viewing angle in the vertical direction ranges from -15° to 15° . Through the angle and distance information, the data is converted into three-dimensional coordinates XYZ values, as shown in Figure 2. The corresponding coordinate conversion formula is:

$$\begin{cases} x = R \cdot \cos \omega \cdot \sin \alpha \\ y = R \cdot \cos \omega \cdot \cos \alpha \\ z = R \cdot \sin \omega \end{cases} \quad (1)$$

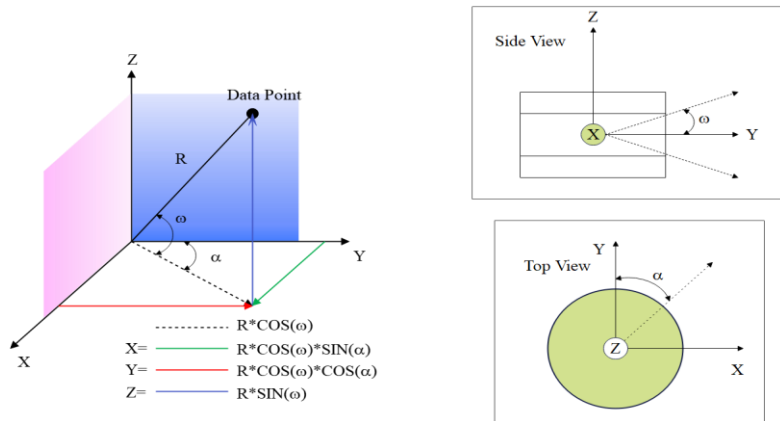


Figure 2: Schematic diagram of laser coordinate conversion.

The image data collection process is responsible for communicating with four high-speed colour industrial cameras and completes colour image data collection through the API provided by the MER125-30G camera provided by Daheng Image. The workflow of the image data collection process is shown in Figure 3.

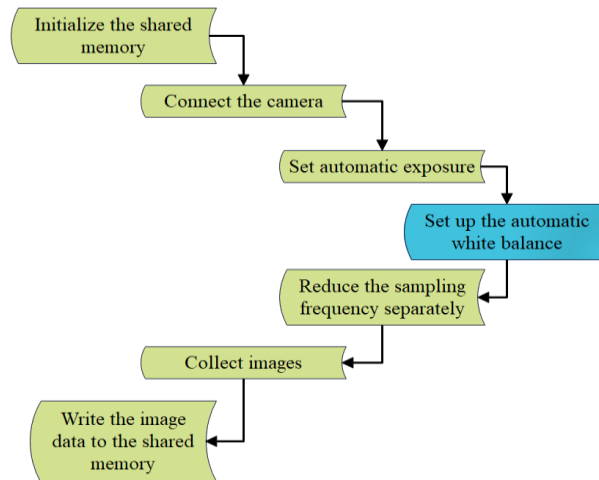


Figure 3: Flowchart of the image collection process.

The workflow of the GPS inertial navigation data collection process is shown in Figure 4. Table 1 records the poses of the panoramic 3D colour laser scanning system corresponding to the three moments. Among them, α , β and γ are the angles between the coordinate axes X_n , Y_n and Z_n under the navigation coordinate system $Ox_nY_nZ_n$ respectively.

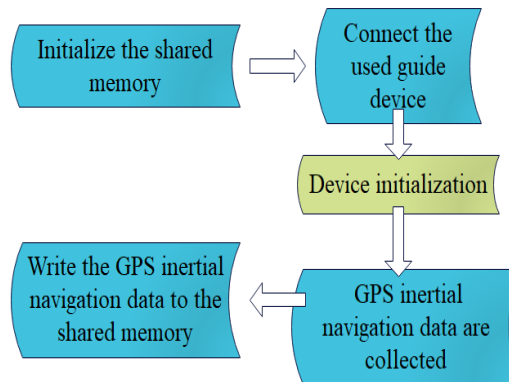


Figure 4: Flow chart of GPS inertial Navigation data collection process.

2.2 Algorithm Layer

The algorithm layer is mainly responsible for data management in shared memory and writing these data to disk. Moreover, it uses the 3D point cloud data, image data, inertial navigation data, and lift platform displacement data in the shared memory to fuse to generate a color point cloud, dense color point cloud, and large-scale scene color 3D point cloud. As shown in Figure 5, they communicate with the driver layer through shared memory and get the data needed to implement the algorithm in the shared memory.

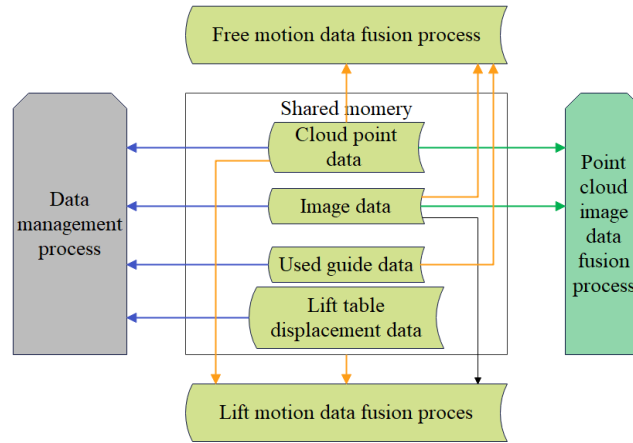


Figure 5: Schematic diagram of data acquisition at the algorithm layer.

Through the three-dimensional laser rangefinder and high-speed colour camera, the geometric mapping relationship between the three-dimensional point cloud in the laser coordinate system and the two-dimensional image in the image coordinate system is solved so as to realize the accurate fusion between the three-dimensional point cloud of the laser rangefinder and the two-dimensional image of the camera. It mainly goes through the following steps:

1. The algorithm makes a black-and-white grid calibration plate.
2. The algorithm collects the 3D point cloud and 2D image of the calibration board.
3. The algorithm performs camera calibration.
4. The algorithm calculates the calibration plate plane in the camera coordinate system.
5. The algorithm establishes the geometric constraints of point and surface.
6. The algorithm establishes geometric constraints of line and surface.
7. The algorithm establishes surface geometric constraints.
8. The algorithm calculates the geometric mapping relationship between the point cloud and the image. The RT matrix is obtained to complete the mapping of the laser point and the camera point:

$$s \begin{bmatrix} u \\ v \\ 1 \end{bmatrix} = A \begin{bmatrix} R & t \end{bmatrix} \begin{bmatrix} x \\ y \\ z \\ 1 \end{bmatrix} \quad (2)$$

The sampling frequency of the GPS-integrated inertial navigation module is much higher than the scanning frequency of the three-dimensional laser rangefinder. Therefore, the linear interpolation method is used to interpolate the device pose information on the time axis to obtain the pose information of the panoramic 3D colour laser scanning system when the point cloud of the frame is collected. The angle α of the X axis in the navigation coordinate system, the angle β of the Y axis, and the angle γ of the Z axis are used to represent the pose information of the system when the

point cloud is collected at frame i . The pose information of the point cloud is used to obtain the rotation matrix R for each frame of the point cloud. The point cloud is rotated to provide a good initial point cloud value for the fusion of multiple scenes and accelerate the point cloud fusion. The device used is a left-handed system, and its rotation matrix is shown below.

$$\begin{aligned}
 R_g &= R_x(\alpha)R_y(\beta)R_z(\gamma) \\
 &= \begin{bmatrix} 1 & 0 & 0 \\ 0 & \cos \alpha & -\sin \alpha \\ 0 & \sin \alpha & \cos \alpha \end{bmatrix} \begin{bmatrix} \cos \beta & 0 & \sin \beta \\ 0 & 1 & 0 \\ -\sin \beta & 0 & \cos \beta \end{bmatrix} \begin{bmatrix} \cos \gamma & -\sin \gamma & 0 \\ \sin \gamma & \cos \gamma & 0 \\ 0 & 0 & 1 \end{bmatrix} \\
 &= \begin{bmatrix} \cos \beta & 0 & \sin \beta \\ \sin \alpha \sin \beta & \cos \alpha & -\sin \alpha \cos \beta \\ -\sin \beta \cos \alpha & \sin \alpha & \cos \alpha \cos \beta \end{bmatrix} \begin{bmatrix} \cos \gamma & -\sin \gamma & 0 \\ \sin \gamma & \cos \gamma & 0 \\ 0 & 0 & 1 \end{bmatrix} \\
 &= \begin{bmatrix} \cos \beta \cos \gamma & -\sin \gamma \cos \beta & \sin \beta \\ \sin \alpha \sin \beta \cos \gamma + \cos \alpha \sin \gamma & -\sin \alpha \sin \beta \sin \gamma + \cos \alpha \cos \gamma & -\sin \alpha \cos \beta \\ -\sin \beta \cos \alpha \cos \gamma + \sin \alpha \sin \gamma & \sin \beta \cos \alpha \sin \gamma + \sin \alpha \cos \gamma & \cos \alpha \cos \beta \end{bmatrix} \quad (3)
 \end{aligned}$$

Then, for the point cloud $P_i = \{p_{i1}, p_{i2}, p_{i3} \dots p_{in}\}$ of the i -th frame, p_{ij} is the j -th point in P_i , and each point in P_i is transformed by the following formula to complete the rotation of the point cloud:

$$p_{ij}^n = R_g p_{ij} \quad (4)$$

The point clouds are then fused using the ICP algorithm. It is known that there are two point clouds P and Q . To convert from the P coordinate system to the Q coordinate system, the rotation and translation matrices R and T need to be calculated. The formula for transformation is:

$$q_i = R p_i + T \quad (5)$$

The ICP algorithm is to minimize the error of the transformation, that is:

$$f(R, T) = \operatorname{argmin} \sum_{i=1}^n \|q_i - (R p_i + T)\|^2 \quad (6)$$

In this paper, the *SVD* method is used to solve the R and T matrices.

1. The algorithm constructs a KD tree and finds the corresponding point pair in the point clouds P and Q to minimize the distance of the i -th point pair, that is to say, to minimize e_i .

$$e_i = q_i - (R p_i + T) \quad (7)$$

2. The algorithm calculates the centroids of point clouds P and Q as:

$$\bar{p} = \frac{1}{n} \sum_{i=1}^n p_i \quad (8)$$

$$\bar{q} = \frac{1}{n} \sum_{i=1}^n q_i \quad (9)$$

Then, there is

$$\begin{aligned} & \sum_{i=1}^n \|q_i - (Rp_i + T)\|^2 \\ &= \sum_{i=1}^n \|q_i - Rp_i - T - \bar{q} + R\bar{p} + \bar{q} - R\bar{p}\|^2 \\ &= \sum_{i=1}^n \|(q_i - \bar{q} - R(p_i - \bar{p})) + (\bar{q} - R\bar{p} - T)\|^2 \end{aligned} \quad (10)$$

$$= \sum_{i=1}^n \left(\|(q_i - \bar{q} - R(p_i - \bar{p}))\|^2 + \|\bar{q} - R\bar{p} - T\|^2 + 2(q_i - \bar{q} - R(p_i - \bar{p}))^T (\bar{q} - R\bar{p} - T) \right)$$

Among them, $q_i - \bar{q} - R(p_i - \bar{p})$ is equal to zero, and the function can be simplified to:

$$f(R, T) = \operatorname{argmin} \sum_{i=1}^n \left(\|q_i - (Rp_i + T)\|^2 + \|\bar{q} - R\bar{p} - T\|^2 \right) \quad (11)$$

2. The algorithm calculates the difference between each point in the point cloud and its centroid, denoted as u_p and u_q :

$$u_p = p_i - \bar{p} \quad (12)$$

$$u_q = q_i - \bar{q} \quad (13)$$

According to the first term of formula (10), it can be optimized to get:

$$R = \operatorname{argmin} \frac{1}{n} \sum_{i=1}^n \|u_q - Ru_p\|^2 \quad (14)$$

Then, the translation matrix T is:

$$T = \bar{q} - R\bar{p} \quad (15)$$

The algorithm is further derived to compute R:

$$\sum_{i=1}^n \|u_q - Ru_p\|^2 = \sum_{i=1}^n (u_q^t u_q + u_p^t R^T R u_p - 2u_q^t R u_p) \quad (16)$$

R is solved using SVD, and the matrix W is defined as follows:

$$W = \frac{1}{n} \sum_{i=1}^n \bar{q} \bar{p}^T \quad (17)$$

The algorithm builds a 4*4 symmetric matrix:

$$Q(W) = \begin{bmatrix} \text{tr}(W) & \Delta \\ \Delta & W + W^T - \text{tr}(W)I_3 \end{bmatrix} \quad (18)$$

Among them, tr is the trace of the matrix and I_3 is the third-order identity matrix.

$$\Delta = [A_{23} A_{31} A_{12}] \quad (19)$$

$$A_{ij} = (W - W^T)_{ij} \quad (20)$$

By solving $Q(W)$, the maximum eigenvalue is calculated, and the unit eigenvector corresponding to the maximum eigenvalue is $q_R = [q_0 \ q_1 \ q_2 \ q_3]^T$, then the final rotation and translation matrix can be transformed into:

$$R(q_R) = \begin{bmatrix} q_0^2 + q_1^2 - q_2^2 - q_3^2 & 2(q_1 q_2 - q_0 q_3) & 2(q_1 q_3 + q_0 q_2) \\ 2(q_1 q_2 + q_0 q_3) & q_0^2 - q_1^2 + q_2^2 - q_3^2 & 2(q_2 q_3 - q_0 q_1) \\ 2(q_1 q_3 + q_0 q_2) & 2(q_2 q_3 + q_0 q_1) & q_0^2 - q_1^2 - q_2^2 + q_3^2 \end{bmatrix} \quad (21)$$

$$q_t = u_q - R(q_R)u_p \quad (22)$$

After the RT matrix is calculated, the transformed point cloud is used as the new source point cloud to continue to iterate until the accuracy is satisfied. If not, repeat the above steps.

1.1 Display Layer

The display layer is mainly responsible for drawing the acquired 3D point cloud and colour image, as well as the display of various data fusion results in the algorithm layer. Each process corresponds to a window, and the arrangement of the windows can be flexibly set.

$P = \{p_i = (x_i, y_i, z_i) / 1 \leq i \leq n\}$ represents an outdoor 3D point cloud scene, and P is a set of discrete points. For a given point P_i in P , we construct a neighbourhood $N_i = \{p_{ij} = (x_{ij}, y_{ij}, z_{ij}) / 1 \leq j \leq m_i\}$ using the KD-Tree algorithm. Then, the covariance matrix M_i is calculated through the neighbourhood N_i of the point P_i .

$$M_i = \sum_{j=1}^{m_i} (p_{ij} - p_i)(p_{ij} - p_i)^T \quad (23)$$

By calculating the covariance matrix M_i , the eigenvalue $\lambda_{i1}, \lambda_{i2}, \lambda_{i3}$ and the eigenvector v_{i1}, v_{i2}, v_{i3} are obtained, where $\lambda_{i1} < \lambda_{i2} < \lambda_{i3}$.

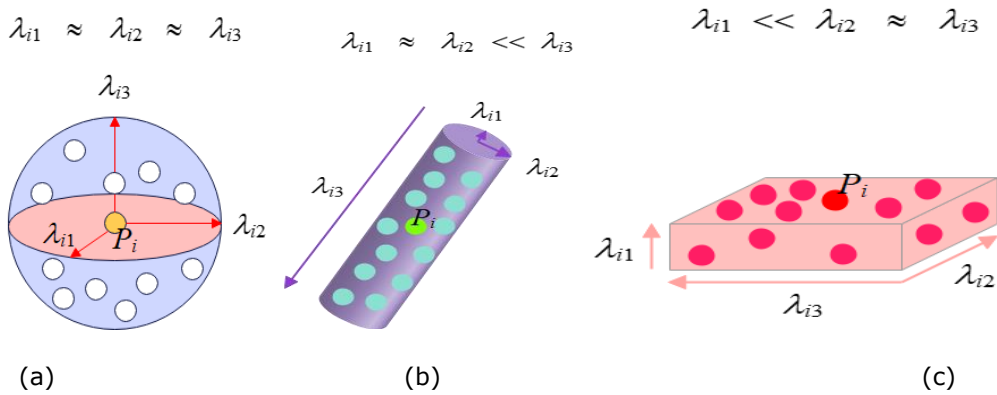


Figure 6: Local shapes and corresponding eigenvalues of (a) circular points, (b) linear points and (c) surface objects.

As shown in Figure 6(a), if $\lambda_{i1} \approx \lambda_{i2} \approx \lambda_{i3}$, the neighbourhood N_i of point P_i is a scattered object, and the point P_i is classified as a circular point. Its basis vector b_i is denoted by v_{i2} , and its scatter feature is denoted by eigenvalue λ_{i3} . As shown in Figure 6(b), if $\lambda_{i1} \approx \lambda_{i2} \ll \lambda_{i3}$, the neighbourhood N_i of the point P_i is a linear object, and the point P_i is classified as a linear point. Its tangent vector t_i is defined as v_{i3} , and its linear characteristic is represented by $\lambda_{i3} - \lambda_{i2}$. As shown in Figure 6(c), if $\lambda_{i1} \ll \lambda_{i2} \approx \lambda_{i3}$, the neighbourhood N_i of point P_i is a planar object, and the point P_i is classified as a planar point. Its normal vector N_i is defined as v_{i1} , and $\lambda_{i2} - \lambda_{i1}$ is used to represent its surface feature.

By using this point cloud local shape analysis method, the three-dimensional point cloud P can be divided into three categories: circular point $P_a = \{p_{ai} / 1 \leq i \leq n_a\}$, linear point $P_b = \{p_{bi} / 1 \leq i \leq n_b\}$ and planar point $P_c = \{p_{ci} / 1 \leq i \leq n_c\}$. Circular points P_a , linear points P_b , and surface objects can be used to represent scattered objects, linear objects, and surface objects in daily life.

Due to the characteristics of mean-shift's non-parametric density estimation, in this paper, the mean-shift algorithm is used to perform hierarchical clustering of the surface objects and linear points on the normal sphere formed by the normal vector $\{n_{ai} / 1 \leq i \leq n_a\}$ of the surface object P_a and the tangent sphere formed by the tangent vector of the linear point. In the mean-shift algorithm, each normal vector n_{ai} on the normal sphere B will keep moving and eventually converge $m(n_{ai}) = \bar{m}(n_{ai}) / |\bar{m}(n_{ai})|$. Among them,

$$\bar{m}(n_{ai}) = \frac{\sum_{j=1}^{\bar{m}_i} G(n_{ai}^j - n_{ai}) n_{ai}^j}{\sum_{j=1}^{m_i} G(n_{ai}^j - n_{ai})} \quad (24)$$

$\{n_{ai}^j / 1 \leq j \leq \bar{m}_i\}$ is a neighbour of n_{ai} , and

$$G(n_{ai}^j - n_{ai}) = \exp\left\{-\frac{|n_{ai}^j - n_{ai}|^2}{2\sigma^2}\right\} \quad (25)$$

It is the spatial distance Gaussian kernel function. Normal vectors n_{ai} that reach the same local maxima of the density function are divided into the same cluster. The normal vectors $N_a = \{n_{ai} / 1 \leq i \leq n_a\}$ of the surface points P_a are gathered into groups $\{N_{ak} / 1 \leq k \leq n_r\}$.

Moreover, each group of normal vectors N_{ak} corresponds to a group of surface points R_{ak} , which are called planar regions. The surface point P_a is divided into a plurality of surface regions $\{R_{ak} / 1 \leq k \leq n_r\}$. Likewise, linear points are clustered in tangential spheres and are divided into multiple linear regions.

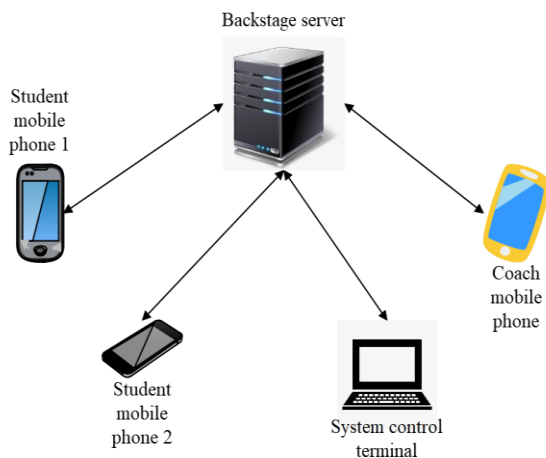
3 DEMONSTRATION METHOD OF SPORTS TRAINING BASED ON MULTIMEDIA TECHNOLOGY

In order to solve the problem of intuitive interaction in online physical education teaching, this research designs a mobile phone online multi-dimensional intuitive interactive sports training system (referred to as an intuitive interactive system) based on VR technology. It can provide coaches and students with an online decentralized, flexible, practical and fully interactive sports training guidance platform.

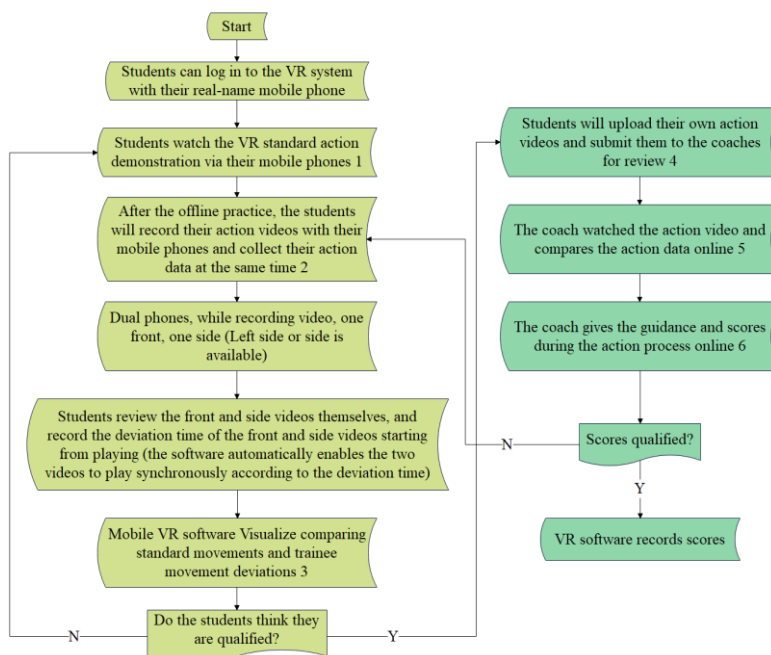
The processing points are as follows. First, students watch standard action demonstrations based on VR technology through mobile phones. After offline practice, students use two mobile phones to collect action videos from the front and side to achieve the effect of three-dimensional capture. Its core steps are as follows. Core Step 1: Two mobile phones simultaneously record the students' action videos, one from the front and one from the side (either left or right). Core step 2: The two mobile phones try to start recording and end at the same time (there may be a deviation of the start time). Core Step 3: Students review the front and side videos by themselves and adjust the playback start time of the two videos to synchronize the actions of the two videos. Moreover, students record the deviation time when the front and side videos start to play (the software system will automatically adjust the two videos according to the deviation time to achieve synchronous playback). Core Step 4: Students upload the front and side videos to the server through the App and enter the deviation time for the front and side videos to start playing in the App system, and the system automatically sends a request for guidance message to the relevant coaches' mobile phones. Second, after receiving the message, the coach logs in to the system and uses a mobile phone (or a common computer terminal) to watch two kinds of student action videos (front and side synchronous playback) in one window at the same time. Third, the coach can pause the playback at any time and insert guidance (voice or text) during the viewing process. Fourth, the coaches enter scores and comments after watching and send them to the students. If the student's movement error is too large or the coach thinks that it does not pass, the student needs to improve the practice offline before submitting. Fifth, the above-mentioned intuitive interaction is performed in a loop until the trainer believes that the student's action has passed. Figure 7(a) is a schematic diagram of the network structure of the intuitive interactive system.

When applied in practice, the intuitive interactive system must be further designed to form a specific implementation scheme. Figure 7(b) shows the implementation flow of the intuitive interactive system.

First, students watch VR standard action demonstrations through mobile phones and use intuitive methods to stimulate their senses, allowing students to practice offline. Second, the mobile phone collects the movements of the students. Students use two cell phones. Third, realize many-to-many intuitive interaction.



(a) Schematic diagram of the network structure of the intuitive interactive system



(b) The implementation process of the intuitive interactive system

Figure 7: Sports training demonstration system based on multimedia technology.

Figure 8 shows the demonstration image of sports training based on multimedia.

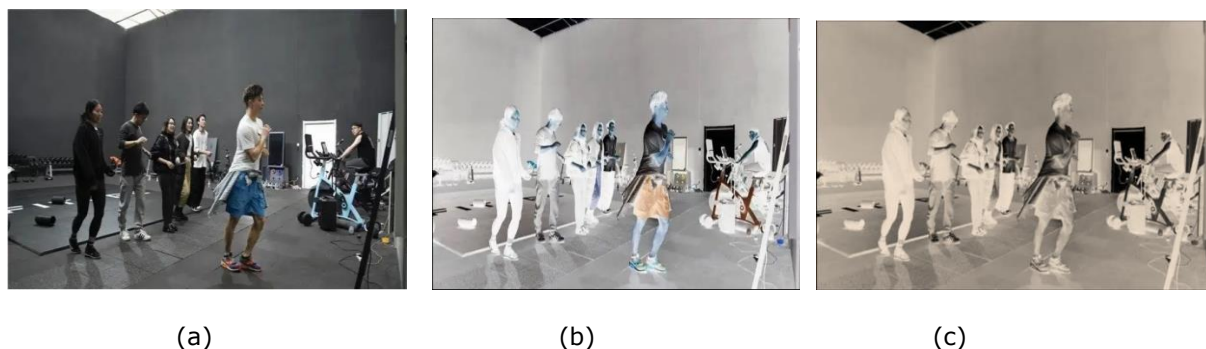


Figure 8: Demonstration image of multimedia sports training: (a) original sports training image, (b) multimedia image processing, (c) multimedia image recognition.

On this basis, the effect of the sports training demonstration method based on multimedia proposed in this paper is tested, and the experimental results shown in Table 1 are obtained through the simulation of multiple sports training groups.

<i>Number</i>	<i>Training effect</i>	<i>Number</i>	<i>Training effect</i>	<i>Number</i>	<i>Training effect</i>
1	85.412	17	84.668	33	82.545
2	82.656	18	80.921	34	87.960
3	87.026	19	82.997	35	81.290
4	81.620	20	82.724	36	85.083
5	79.133	21	86.380	37	80.367
6	82.862	22	79.388	38	80.908
7	79.067	23	81.141	39	82.584
8	84.499	24	87.674	40	79.328
9	86.407	25	85.956	41	82.029
10	84.376	26	84.543	42	82.590
11	81.339	27	87.779	43	87.949
12	82.650	28	86.282	44	86.723
13	87.900	29	79.380	45	81.696
14	86.041	30	83.904	46	81.756
15	85.237	31	86.266	47	85.949
16	87.939	32	79.905	48	85.126

Table 1: Verification of the effect of sports training demonstration method based on multimedia.

The results of the sports training simulation verify that the sports training demonstration method based on multimedia works very well.

4 CONCLUSIONS

In the application of modern information technology teaching, the computer is mainly used to convert specific theoretical knowledge and demonstration actions into digital processing, output, and simulation through the skills information of text, pictures, and audio-visual video. We can also purposefully correct, filter, and delete unnecessary information, and the obtained information will be easier to understand. Compared with the traditional conventional teaching mode, information-based teaching can update the teaching mode in time and improve the teaching effect. It can be decomposed into the overall teaching process of skills so that athletes can learn each skill during

training. This not only improves the operability of skill learning but also reduces training time and enhances trainers' confidence and interest in sports training. This paper combines multimedia technology to study the demonstration method of sports training. The results of the sports training simulation verify that the sports training demonstration method based on multimedia works very well. The integration of Collaborative CAD multimedia technology demonstrations has opened new horizons in the field of athletic development. This project represents a pioneering effort to leverage the transformative capabilities of 5G technology and multimedia applications to elevate sports training to unprecedented levels of effectiveness, efficiency, and engagement.

Chungen Zhang , <https://orcid.org/0009-0000-5026-4977>

REFERENCES

- [1] Azhand, A.; Rabe, S.; Müller, S.; Sattler, I.; Heimann-Steinert, A.: Algorithm Based on One Monocular Video Delivers Highly Valid and Reliable Gait Parameters, *Scientific Reports*, 11(1), 2021, 1-10. <https://doi.org/10.1038/s41598-021-93530-z>
- [2] Bakshi, A.; Sheikh, D.; Ansari, Y.; Sharma, C.; Naik, H.: Pose Estimate Based Yoga Instructor, *International Journal of Recent Advances in Multidisciplinary Topics*, 2(2), 2021, 70-73.
- [3] Bhombe, J.; Jethwa, A.; Singh, A.; Nagarhalli, T.: Review of Pose Recognition Systems, *VIVA-Tech International Journal for Research and Innovation*, 1(4), 2021, 1-8.
- [4] Colyer, S. L.; Evans, M.; Cosker, D. P.; Salo, A. I.: A Review of the Evolution of Vision-Based Motion Analysis and the Integration of Advanced Computer Vision Methods Towards Developing a Markerless System, *Sports Medicine-Open*, 4(1), 2018, 1-15. <https://doi.org/10.1186/s40798-018-0139-y>
- [5] Díaz, R. G.; Laamarti, F.; El Saddik, A.: DTCoach: Your Digital Twin Coach on the Edge During COVID-19 and Beyond, *IEEE Instrumentation & Measurement Magazine*, 24(6), 2021, 22-28. <https://doi.org/10.1109/MIM.2021.9513635>
- [6] Ershadi-Nasab, S.; Noury, E.; Kasaei, S.; Sanaei, E.: Multiple Human 3d Pose Estimation From Multiview Images, *Multimedia Tools and Applications*, 77(12), 2018, 15573-15601. <https://doi.org/10.1007/s11042-017-5133-8>
- [7] Li, Z.; Bao, J.; Liu, T.; Jiacheng, W.: Judging the Normativity of PAF Based on TFN and NAN, *Journal of Shanghai Jiaotong University (Science)*, 25(5), 2020, 569-577. <https://doi.org/10.1007/s12204-020-2177-0>
- [8] Liu, J. J.; Newman, J.; Lee, D. J.: Using Artificial Intelligence to Provide Visual Feedback for Golf Swing Training, *Electronic Imaging*, 2021(6), 2021, 321-1. <https://doi.org/10.2352/ISSN.2470-1173.2021.6.IRIACV-321>
- [9] McNally, W.; Wong, A.; McPhee, J.: Action Recognition using Deep Convolutional Neural Networks and Compressed Spatio-Temporal Pose Encodings, *Journal of Computational Vision and Imaging Systems*, 4(1), 2018, 3-3.
- [10] NagalakshmiVallabhaneni, D. P. P.: The Analysis of the Impact of Yoga on Healthcare and Conventional Strategies for Human Pose Recognition, *Turkish Journal of Computer and Mathematics Education*, 12(6), 2021, 1772-1783. <https://doi.org/10.17762/turcomat.v12i6.4032>
- [11] Nie, X.; Feng, J.; Xing, J.; Xiao, S.; Yan, S.: Hierarchical contextual Refinement Networks for Human Pose Estimation, *IEEE Transactions on Image Processing*, 28(2), 2018, 924-936. <https://doi.org/10.1109/TIP.2018.2872628>
- [12] Nie, Y.; Lee, J.; Yoon, S.; Park, D. S.: A Multi-Stage Convolution Machine with Scaling and Dilation for Human Pose Estimation, *KSII Transactions on Internet and Information Systems (TIIS)*, 13(6), 2019, 3182-3198. <https://doi.org/10.3837/tiis.2019.06.023>

- [13] Sáráandi, I.; Linder, T.; Arras, K. O.; Leibe, B.: Metrabs: Metric-scale Truncation-Robust Heatmaps for Absolute 3d Human Pose Estimation, *IEEE Transactions on Biometrics, Behavior, and Identity Science*, 3(1), 2020, 16-30. <https://doi.org/10.1109/TBIOM.2020.3037257>
- [14] Xu, J.; Tasaka, K.: Keep Your Eye On the Ball: Detection of kicking Motions in Multi-View 4K Soccer Videos, *ITE Transactions on Media Technology and Applications*, 8(2), 2020, 81-88. <https://doi.org/10.3169/mta.8.81>
- [15] Zarkeshev, A.; Csiszár, C.: Rescue Method Based on V2X Communication and Human Pose Estimation, *PeriodicaPolytechnica Civil Engineering*, 63(4), 2019, 1139-1146. <https://doi.org/10.3311/PPci.13861>